Raman scattering in $PbZr_{1-x}Ti_xO_3$ single crystals with low Ti content and a study of the Ti influence

1989 J. Phys.: Condens. Matter 1 2257

(http://iopscience.iop.org/0953-8984/1/12/010)

J. Phys.: Condens. Matter 1 (1989) 2257–2268. Printed in the UK

Raman scattering in $PbZr_{1-x}Ti_xO_3$ single crystals with low Ti content and a study of the Ti influence

K Roleder†, G E Kugel‡, M D Fontana‡, J Handerek†, S Lahlou‡ and C Carabatos-Nédelec†

† Institute of Physics, University of Silesia, 40-007 Katowice, ul. Uniwersytecka 4, Poland

‡ Centre Lorrain d'Optique et Electronique des Solides Université de Metz, Supelec, Technopole de Metz 2000, 2 rue Edouard Belin, 57078 Metz Cédex 3, France

Received 2 June 1988

Abstract. Investigations of the Raman scattering spectra of $PbZr_{0.99}Ti_{0.01}O_3$ single crystals were performed over a large temperature range from 10 to 650 K and compared with those of pure $PbZrO_3$. The main modifications of the Raman spectra have been found to appear near the transitions between the antiferroelectric–intermediate and the intermediate–para-electric phases. In particular, a polarisation effect of the light scattering in the para-electric phase has been detected and attributed to the special role of Ti ions introduced in the host lattice of lead zirconate. These ions can be regarded as defects breaking the local symmetry and leading to the creation of polar clusters in the para-electric phase. Below a defined temperature in this phase, a long-range interaction appears and causes cluster ordering. The change in the Raman spectra and in the light scattering intensity and polarisation is analysed and connected with the dielectric and pyroelectric properties investigated on the same sample.

1. Introduction

Pure lead zirconate $PbZrO_3$ as well as solid solutions of $PbZr_{1-x}Ti_xO_3$ (PZT) with a small Ti concentration ($x < 0.06$) are well known as typical materials displaying an antiferroelectric structure in the low-temperature phase. The space group and point group of the antiferroelectric phase were determined as P*ba*m and mmm, respectively (Fujishita and Hoshino 1984). These compounds have been, in the last few decades, extensively investigated by structural, dielectric, pyroelectric and electromechanical experimental methods (Sawaguchi 1953, Handerek and Ujma 1977, Whatmore *et al* 1978, Morozov *et al* 1978, Roleder 1980, 1988, Handerek *et al* 1985). Moreover, the solid solutions with a high Ti concentration have been used in many practical applications owing to their excellent electromechanical properties.

From the scientific point of view, many papers concerned mainly the existence and the nature of the intermediate phase (I) below the T_c point between the antiferroelectric (A) and para-electric (P) phases in pure $PbZrO_3$ and in the $PbZr_{1-x}Ti_xO_3$ ($x < 0.06$) solutions. Most researchers confirmed the presence of a transient phase, in which ferroelectric behaviour occurs, in both ceramics and single crystals. The space group of the intermediate phase was found to be F2mm (Tanaka *et al* 1982). It is well established that the non-stoichiometry in the Pb and O sublattices strongly influences the properties of these materials (Ujma 1984). Recent investigations on thin $PbZrO_3$ single crystals

0953-8984/89/122257 + 12 $02.50

revealed that the transient phase does not develop spontaneously but results from defects caused by a high external electric field or separation of point defects by a field (Roleder and Dec 1989). In the case of thick (greater than 0.5 mm) crystals and probably because of their imperfections and inhomogeneities, a transient phase was clearly observed which was independent of the different technological growing processes employed.

In spite of the strong influence of the non-stoichiometry on the $PbZrO_3$ properties, in many papers the introduction of foreign ions in place of Pb and Zr have been dealt with. Among ions such as Ba, Ca, La, Ti, Sn and Hf, the Ti ion in particular radically changes the properties of solid solutions obtained in this way. Also, the Ti ions extend significantly the temperature range of the intermediate-phase existence towards lower temperatures. Moreover, the phase diagrams of PZT obtained from different measurement methods are controversial. At present, one can distinguish two critical points at Ti concentrations $x = 0.02$–0.03 (Sawaguchi 1953, Roleder 1988) and $x = 0.06$ (Whatmore *et al* 1978). Above the critical concentration $x = 0.06$, the crystals exhibit only the ferroelectric state below T_c.

In contrast with the number of dielectric, structural and electromechanical investigations and certainly because of difficulties in obtaining crystals of sufficiently good quality for optical studies, experimental Raman spectroscopy studies are rather scarce. Pasto and Condrate (1973) measured the Raman spectra on powders and multi-domain single crystals of $PbZrO_3$ from room temperature to 250 °C. They interpreted the results within the framework of a factor group analysis and considered only the antiferroelectric–para-electric transition, ignoring the existence of an intermediate phase. Some Raman data on the PZT solid solutions are available but concern essentially results on ceramic samples with the Ti content x greater than 0.10 (Bauerle and Pinczuk 1976, Bauerle *et al* 1974, 1977). In the rhombohedral PZT, as in $PbTiO_3$, an E(TO) mode was found to soften with increasing temperature and also with increasing Ti concentration. This mode was correlated with the ferroelectric–para-electric phase transition.

The aim of this paper is to reinvestigate the Raman spectra of pure $PbZrO_3$ and PZT with low Ti concentration using single crystals of sufficiently good quality. Furthermore, we relate Raman data to the structural phase transition sequence and especially to the existence of the intermediate phase. This intermediate phase has been proved to exist in large-sized $PbZrO_3$ crystals which we have preliminarily investigated by Raman spectroscopy (Roleder *et al* 1987). Since a small number of Ti ions changes markedly the dielectric properties of pure $PbZrO_3$ (Roleder 1989), we chose a plate of $PbZr_{1-x}Ti_xO_3$ with x about 0.01 (PZT1) which belongs to the first critical region below $x = 0.02$–0.03. Particular attention was paid to investigation of the para-electric phase.

2. Experimental details

Our investigations were performed on crystals produced by the modified method used by Scott and Burns (1972). A rectangular $PbZrO_3$ crystal of light-red colour was chosen. This crystal possessed a multi-domain structure below the cubic phase. The PZT1 sample was a transparent plate of 0.3 mm thickness and of light-red colour. The concentration of Ti ions of about 1 mol.% ($x = 0.01$) in the sample was established by comparing the dielectric behaviour, especially in the para-electric phase, with other PZT crystals investigated by x-ray microanalysis. Under a polarising microscope, this sample revealed a reproducible single-domain state in the antiferroelectric orthorhombic phase. The c axis of this phase was perpendicular to the plate surface.

Table 1. Raman tensors and the irreducible representations measured by the scattering geometries used. k_i and k_f are the wavevectors of the incident and scattered light, respectively.

k_i	k_f	Raman tensor	Irreducible representation
x	y	yx	A_g, B_{1g}
x	y	zz	A_g
x	y	yz	B_{2g}, B_{3g}
x	y	zx	B_{2g}, B_{3g}
x	z	yy	B_{1g}, A_g
x	z	yx	B_{1g}, A_g
x	z	zy	B_{2g}, B_{3g}
x	z	zx	B_{2g}, B_{3g}

The experiments were carried out on a Spex double-monochromator model 1401, using a photon-counting system and linked with a Datamate microprocessed spectrometer controller and data acquisition. For the measurements between room temperature and high temperatures, the sample was mounted in a temperature-controlled furnace. The low-temperature spectra were recorded with the crystal placed in an Air-Product Displex cryostat driven with an automatic indicator controller. The Raman measurements were carried out from 10 to 650 K. In order to control the phase transition temperature, we performed, simultaneously with the Raman recording, measurement of the electric permittivity. For the Raman measurements, especially for PZT1, we adopted the following orientational notations: the z axis is taken perpendicular to the plate surface which corresponds to the c axis of the orthorhombic crystal structure. The x and y axes are chosen along the crystal edges and bisect the true orthorhombic a and b unit-cell axes. According to this convention, we present in table 1 the irreducible representations and the Raman susceptibility tensors reached with the indicated scattering geometry.

3. Raman results and analysis

3.1. General Raman spectra of $PbZrO_3$ *and* PZT1

In order to compare the complete Raman spectra for pure $PbZrO_3$ and PZT1, we represent in figure 1 four spectra recorded between 0 and 800 cm^{-1}. The non-polarised spectrum in figure 1(a) is for $PbZrO_3$ at room temperature; the spectra in figures 1(b) and 1(c) are for PZT1 in the scattering configurations $x(yy)z$ and $x(zz)y$, respectively; the spectrum in figure 1(d) corresponds to the low-temperature spectrum in the $x(yy)z$ configuration for PZT1.

In the room-temperature spectra, one can clearly distinguish three main frequency regions I, II and III extending over 0–200 cm^{-1}, 200–400 cm^{-1} and 400–800 cm^{-1}, respectively. These regions are common features of the oxide perovskite crystal families. The origin of these regions can be analysed within the framework of the phonon dispersion behaviour known in the cubic phase of similar perovskite crystals. The lowest-frequency range I, which contains lines of high intensity, involves phonons corresponding to the lowest-frequency optic and acoustic branches activated by the antiferrodistortive transition, leading to the antiferroelectric structure. The next two regions arise from the splittings and activations of the higher-frequency phonons of this transition. Comparison

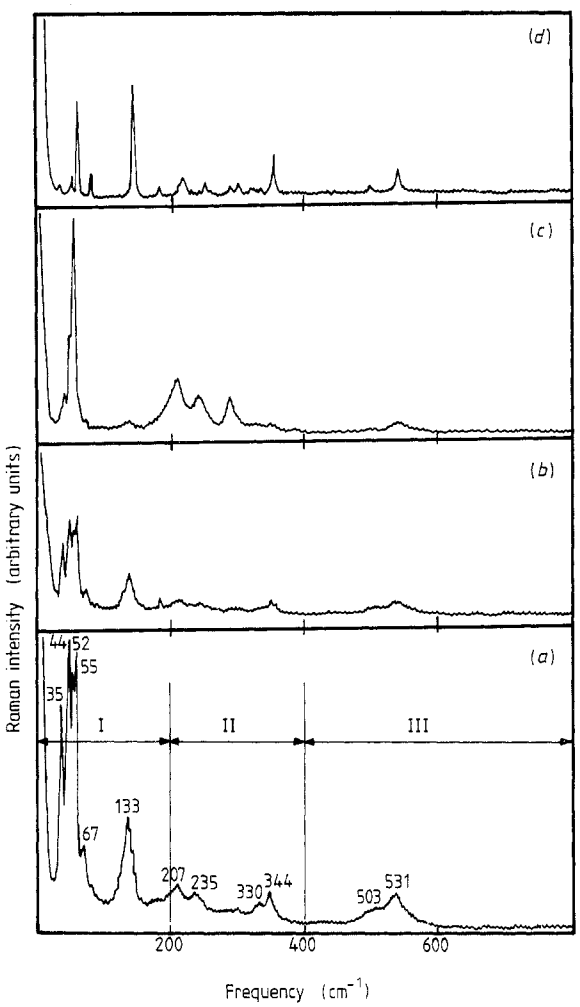

Figure 1. Comparison of the Raman spectra of $PbZrO_3$ and PZT1: (*a*) the non-polarised room-temperature (300 K) spectrum of $PbZrO_3$; (*b*) polarised room-temperature (300 K) spectrum for PZT1, $x(yy)z$ configuration; (*c*) polarised room-temperature (300 K) spectrum for PZT1, $x(zz)y$ configuration; (*d*) low-temperature (10 K) polarised spectrum for PZT1, $x(yy)z$ configuration.

of the spectral line positions in figures 1(*a*)–(*c*) indicates that the introduction of a small Ti concentration does not significantly modify the Raman spectra in the antiferroelectric phase.

Comparison of the polarised Raman spectrum in figure 1(*b*) with that in figure 1(*c*), showing the strong decrease in the intensity of the structure at 133 cm^{-1} and significant enhancement of the spectral region II, reveals the single-domain character of the PZT1 sample. Similar experiments on several $PbZrO_3$ samples failed and thus revealed the multi-domain character of samples.

Since in the antiferroelectric phase the unit cell of $PbZrO_3$ contains eight formula units, a maximum of 117 optic phonons should exist at room temperature and low temperatures. The spectrum recorded at 10 K (figure 1(*d*)) displays only about 30 peaks of various intensities and is better resolved than at room temperature.

3.2. Polarised low-temperature Raman spectra for PZT1 crystal

Of the several scattering geometries investigated (table 1), we represent in figure 2 four spectra labelled A, B, C and D corresponding to the $x(zz)y$, $x(yy)z$, $x(yx)y$ and $x(zy)z$

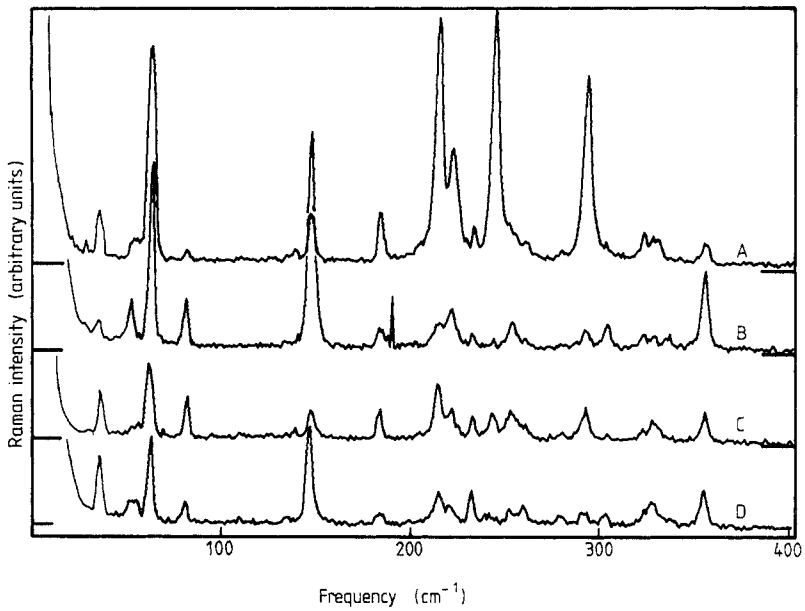

Figure 2. Low-temperature (10 K) Raman spectra of PZT1 detected for various scattering geometries: spectrum A, $x(zz)y$; spectrum B, $x(yy)z$; spectrum C, $x(yx)y$; spectrum D, $x(zy)z$.

scattering configurations, respectively, and recorded in the frequency range from 0 to 400 cm^{-1}. Because of the low symmetry of the crystal structure and the large number of atoms in the unit cell, all symmetry components exhibit numerous phonon peaks. Comparison of spectra A and C in figure 2 allows us to assign the structure at 80 and 252 cm^{-1} to the B_{1g} symmetry. Furthermore, the scattering intensity of the $x(zz)y$ configuration (figure 2, spectrum A) is higher than that of the $x(yx)y$ configuration (figure 2, spectrum C). This indicates the higher value of the zz susceptibility Raman tensor.

The temperature dependence of the various Raman scattering geometries between 10 K and room temperature does not exhibit abnormal modification in the line positions and their widths. This shows the non-existence of a further phase transition below room temperature.

3.3. Temperature dependence of Raman spectra from room temperature to the antiferroelectric–intermediate phase transition in PZT1

In PZT1, as well as in $PbZrO_3$, an intermediate phase was observed. In this phase the coexistence of antiferroelectric, ferroelectric and para-electric states has been detected previously (see, e.g., Tennery 1965, Handerek *et al* 1985). In this section, we describe the polarised Raman spectra and its temperature dependence in the low-frequency range 0–200 cm^{-1} when approaching this specific phase. Figure 3 presents the spectra from room temperature to the A–I transition temperature T_{A-I} for the scattering geometries used. Our results point out that the lowest-phonon-frequency band at 35 cm^{-1} clearly shows a polarised character. This line is almost non-existent for the $x(zy)z$ configuration (figure 3(d)) at room temperature. Similarly the line at 44 cm^{-1} is absent for the $x(yx)y$ geometry.

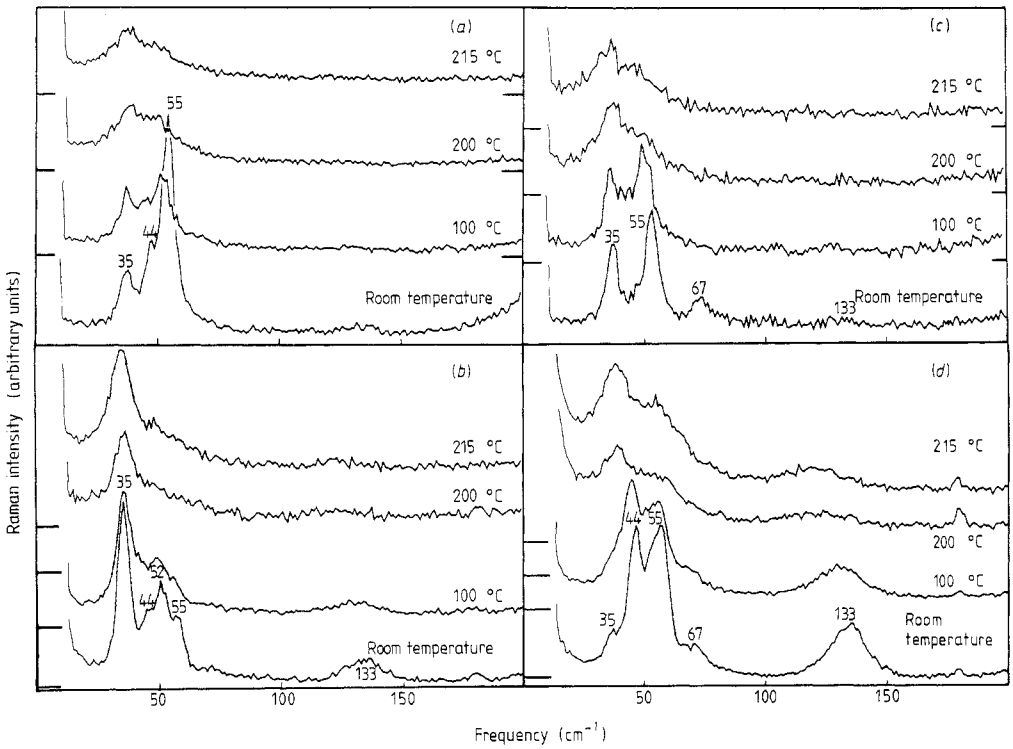

Figure 3. Temperature-dependent Raman spectra of PZT1 in the low-frequency range below T_{A-I} for various scattering geometries: (*a*) $x(zz)y$; (*b*) $x(yy)z$; (*c*) $x(yx)y$; (*d*) $x(zy)z$.

With increasing temperature, as already observed in pure $PbZrO_3$, the lowest-frequency peak at 35 cm^{-1} remains stable in contrast with the peak at 44 cm^{-1} which softens gradually with increasing temperature towards the previously mentioned line (figure 3(*d*)). The structures at 52, 55 and 67 cm^{-1} decrease in intensity and finally form a broad shoulder. The line at 133 cm^{-1}, observed in the $x(zy)z$ and $x(yy)z$ configurations only, noticeably softens and broadens above 200 °C.

Although the effect of light scattering polarisation in the peak positions and line-shapes disappears at temperatures above 200 °C, there is a drastic difference in the intensity of quasi-elastic scattering for each temperature below T_{A-I}. This is clearly illustrated in figure 4.

3.4. Transition from the antiferroelectric phase to the intermediate phase and spectra in the intermediate phase

As mentioned in § 2, all the Raman experiments above room temperature have been accompanied by simultaneous permittivity observation. The temperature dependence of ε in the vicinity of phase transitions is plotted in figure 5. The transition temperatures T_{A-I} and T_{I-A} correspond to the points at which ε starts to show a marked increase on heating or approaches a region of weak dependence on cooling. This assignment was made on the basis of changes in the Raman spectra at these temperatures (figure 6(*a*)). Indeed, at the T_{A-I} point the remaining antiferroelectric phase bands disappear and above T_{A-I} the Raman spectra contain a broad shoulder only. The same behaviour was

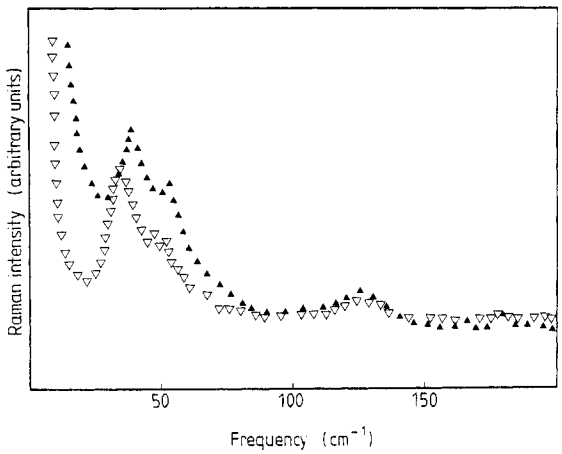

Figure 4. Low-frequency Raman spectra for PZT1 at 150 °C for $x(zy)z$ (▲) and $x(yy)z$ (▽) configurations. The difference in the quasi-elastic scattering intensity is clearly observed.

detected for $PbZrO_3$. The origin of the broad shoulder in the intermediate phase can be attributed to strongly overdamped phonons. Inside the intermediate phase, no light polarisation effect was observed (figure 6(*b*)). This may be explained by the coexistence of the phases and the occurrence of a multi-domain structure, observed under a polarising microscope, in this temperature region. Approaching the T_{I-P} point, which corresponds to the ε_{max} value, the intensity of the Raman spectra, especially of the quasi-elastic contribution, is clearly modified. In the $x(zy)z$ configuration, as shown in figure 7, the intensity strongly increases while for the $x(yy)z$ configuration an equivalent decrease is observed.

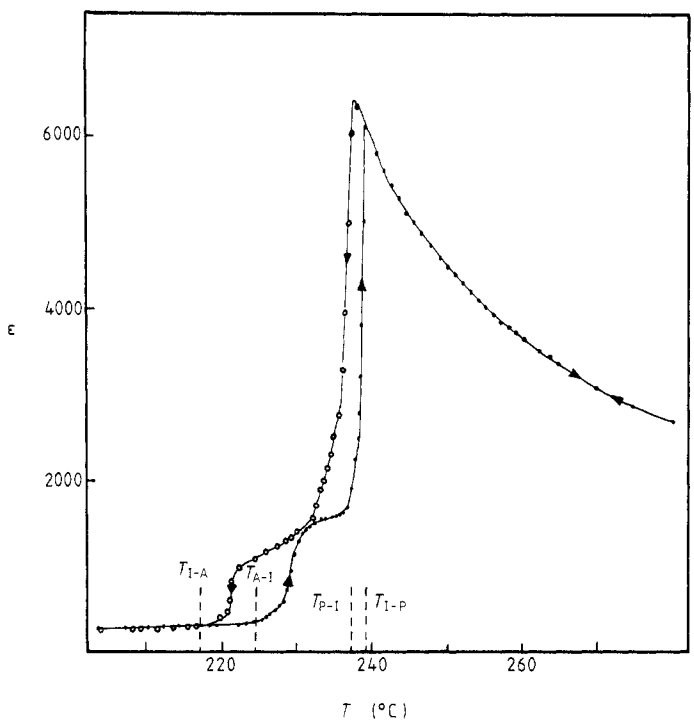

Figure 5. Temperature dependence of the permittivity (1 kHz, 0.1 kV cm^{-1}) for PZT1 near the phase transitions.

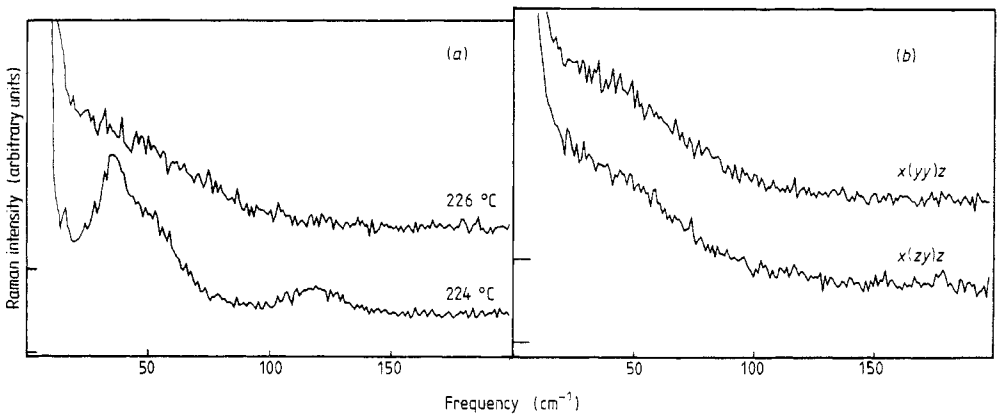

Figure 6. Low-frequency Raman spectra in the vicinity of T_{A-I}: (*a*) spectra slightly below and above T_{A-I} (225 °C), $x(zy)z$ scattering geometry; (*b*) two spectra with different scattering geometries in the intermediate phase (232 °C). (Note the base-line shift.)

3.5. Transition from the intermediate to the para-electric phase and spectra in the para-electric phase

In contradiction to those obtained near T_{A-I}, the Raman spectra do not change drastically at T_{I-P} except for a small and continuous decrease in the scattered intensity especially for the $x(zy)z$ geometry. In contrast with pure $PbZrO_3$, for the PZT1 crystal the characteristic broad shoulder observed in the transient phase is still present above $T_{\varepsilon_{max}}$. This shoulder does not disappear even at higher temperatures. Similar features have already been observed for a PZT sample with a higher concentration of Ti (Bauerle and Pinczuk 1976) and seem to be exclusively connected with the introduction of Ti into the host lattice of $PbZrO_3$.

A further interesting fact emerging from our experiments is the clear light polarisation effect of the Raman spectra in the cubic para-electric phase of PZT1. Figure 8 gives a comparison between the $x(zz)y$ and $x(yz)y$ spectra, illustrating this unusual polarisation effect at 275 °C. The increase in temperature above 275 °C inside the para-electric phase yields a continuous decrease in the quasi-elastic scattering intensity for the $x(zz)y$ geometry (figure 9(*a*)) and no significant modification for the $x(yz)y$ geometry (figure 9(*b*)).

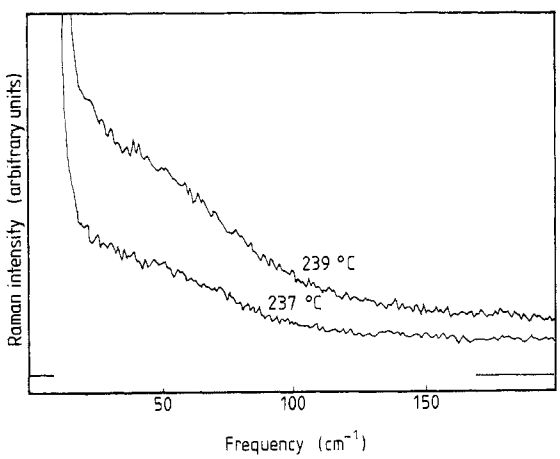

Figure 7. Change of the quasi-elastic scattering intensity for the $x(zy)z$ geometry below T_{I-P}.

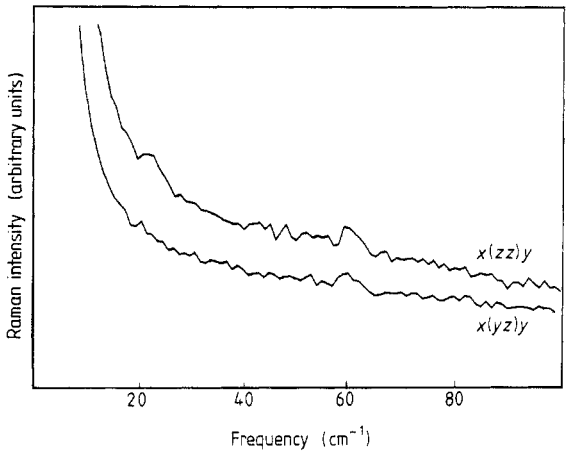

Figure 8. Polarisation effect of the quasi-elastic diffusion in the para-electric phase for PZT1 at 275 °C.

In order to determine the physical origin of the temperature dependence of the central component and of the polarisation effect in the Raman spectra, some supplementary Raman experiments have been performed in an electric field on an additional PZT sample. The corresponding results are reported in § 4 to support the interpretation of the results presented up to now.

4. Interpretation of results and discussion

In order to illustrate the main effects observed in the light scattering experiments and to connect them with the dielectric properties, we represent in figure 10 the electric permittivity ε recorded simultaneously with the light scattering intensity at a frequency of 15 cm^{-1} as a function of temperature. The pyroelectric effect for a non-polarised sample is also included in the discussion.

In order to interpret the various effects detected, it is more convenient to start the

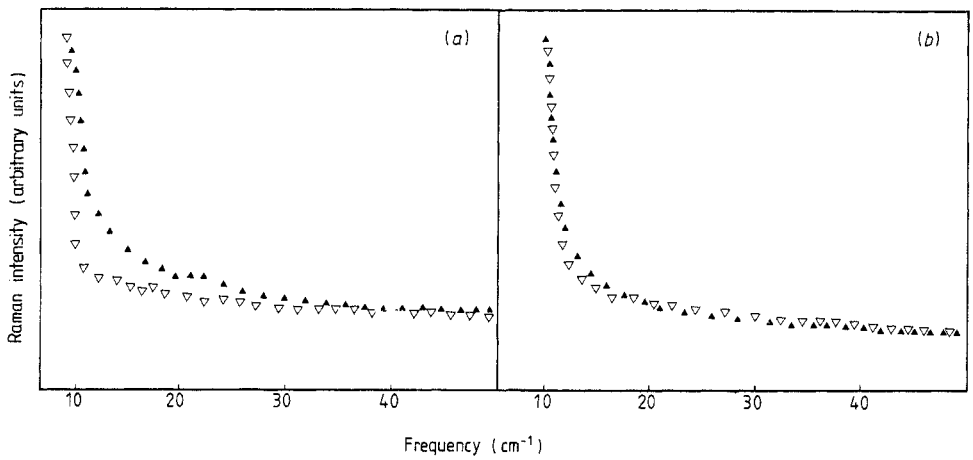

Figure 9. Temperature dependence of the quasi-elastic diffusion in the para-electric phase for (*a*) the $x(zz)y$ and (*b*) the $x(yx)y$ configurations: ▲, 275 °C; ▽, 330 °C.

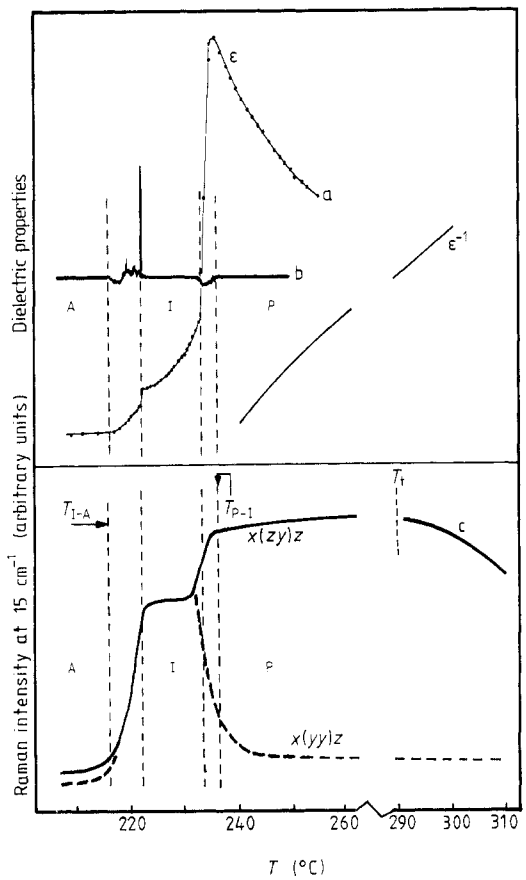

Figure 10. Schematic view of the temperature dependence of the electric permittivity (curve a), the pyroelectric current detected on a virgin sample (curve b), and the light scattering intensity recorded at 15 cm^{-1} (curve c) in the cooling process for two configurations.

discussion from the high-temperature side. At sufficiently high temperatures, above $T_t = T_{P-I} + 50\,°C$, the sample seems to possess a para-electric state since no anisotropy appears in the scattering. In this region, $\varepsilon^{-1}(T)$ obeys the classical Curie–Weiss law. Below T_t a deviation from the Curie–Weiss law is accompanied by an additional polarity detected by the pyroelectric method (Roleder 1989). Since in this region the light polarisation effect of the quasi-elastic diffusion appears, we believe that the origins of these phenomena are the same, for instance the existence of polar regions above T_{P-I}. To verify this assumption, we studied the influence of the external electric field on the quasi-elastic diffusion intensity in order to modify the possible ordering of these polar clusters. We chose for this experiment another larger PZT crystal of comparable Ti concentration, about 1.5 mol.% ($x = 0.015$). Electrodes were deposited perpendicular to the c axis. Dielectric and Raman scattering tests confirmed a behaviour similar to that of PZT1. The quasi-elastic scattering intensity was then observed for $x(zz)y$ and $x(yx)y$ geometries within the temperature range $T_{P-I} < T < T_t$. Without an external field, as for the PZT1 crystal, there was a clear polarisation effect; the intensity of scattered light for the $x(zz)y$ geometry was considerably greater than for the $x(yx)y$ geometry. In a DC electric field of strength 1.5 kV cm^{-1} a small, but evident, increase in quasi-elastic intensity was observed for the $x(zz)y$ configuration. As shown in figure 11, a further increase in the field strength (e.g. 3 kV cm^{-1}) leads to the saturation effect; no change in the quasi-elastic scattering shape and intensity was observed for stronger fields. Simultaneously, no modification of the scattering intensity in a electric field was observed

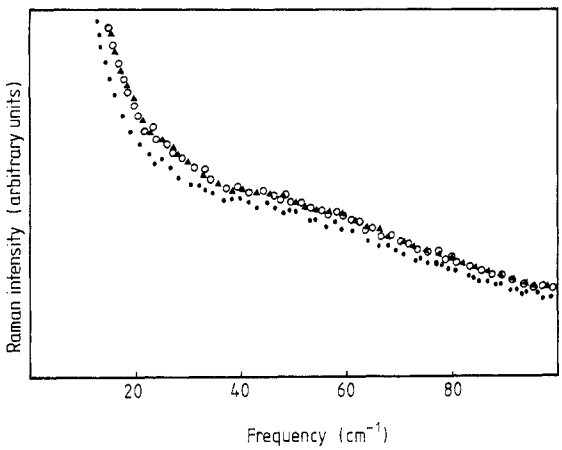

Figure 11. Influence of an external DC electric field on the quasi-elastic scattering intensity inside the para-electric phase at 275 °C ($x(zz)y$ scattering geometry): ●, 0 kV cm^{-1}; ○, 1.5 kV cm^{-1}; ▲, 3 kV cm^{-1}.

for the $x(yx)y$ geometry. Hence, in the investigated PZT crystal, we can speak about polarised quasi-elastic scattering above T_{P-I} caused by the existence of polar regions the ordering of which can be modified with an external DC field. Since the effect of polarisation exists even in the virgin PZT crystal, one can conclude that these polar regions are not randomly distributed but preponderantly ordered in a defined direction (the c axis in our convention). The external electric field only improves their alignment. Above T_t the polar region ordering is no longer persistent and consequently the polarisation effect vanishes.

Below T_{P-I} (ε_{max}), the intermediate phase is formed (figure 10) and thus pyroelectric current pulses are observed. At the same time the polarisation effect of the light scattering disappears. In this intermediate phase region, where pyroelectric currents are absent, only a continuous decrease in ε takes place. This temperature region is characterised by a complex domain structure and coexistence of ferroelectric and antiferroelectric phases. Since, as shown before, the polar regions above T_{P-I} are oriented along the c axis and the 'anti-polarisation' vector in the low-temperature antiferroelectric phase takes a direction p in the a–b plane (Dec 1988), the complex structural character of this intermediate phase is easily created. Moreover, an enlargement of the polar regions in the intermediate phase region may take place. Going towards the antiferroelectric phase, the pyroelectric pulses appear again with a stronger magnitude than those just below the T_{P-I} point. Their appearance is accompanied by a decrease in the light scattering intensity again with a detectable polarisation effect. As shown in § 2, this decrease in the light scattering at 15 cm^{-1} through the T_{I-A} transition is connected with the disappearance of the broad band characteristic of the intermediate phase, and with the appearance of better resolved phonon peaks located near 35 cm^{-1} (see figure 6). All the effects presented in figure 10 allow the phase transition points to be accurately determined and are similar in heating and cooling processes with those desired for the thermal hysteresis effect.

The main conclusion which can be drawn from these measurements is that the Ti ions introduced into the lattice of pure $PbZrO_3$ can be regarded as defects breaking the local symmetry and leading therefore to first-order Raman scattering in the para-electric phase, as a remaining broad band. Furthermore, the presence of Ti initiates the creation of polar clusters which are, to some degree, ordered within the defined temperature region $T_{P-I} < T < T_t$. Above T_t, these clusters are randomly distributed. Because of the possible non-stoichiometry of the crystals investigated, we cannot exclude the inter-

actions of the Ti ions with the defects in the Pb and O sublattices which are known to influence the ferroelectric properties of the intermediate phase in $PbZrO_3$ but which are unable to induce a polarity in the para-electric phase. Moreover, the existence of polar regions above T_{I-P} seems to stimulate the mechanism governing the appearance of the intermediate phase and is probably responsible for the reproducible formation of the single-domain structure in the antiferroelectric phase.

First-order Raman scattering in the para-electric phase was also observed for solid $PbZr_{1-x}Ti_xO_3$ solutions with a high Ti content $x = 0.10$ (Bauerle and Pinczuk 1976). Recently, infrared reflectivity spectroscopy revealed that the local symmetry in the para-electric phase of $PbZr_{0.75}Ti_{0.25}O_3$ ceramic is lower than that of the cubic phase (Zelezny *et al* 1988). Hence, we can conclude that any Ti content introduced into the $PbZrO_3$ lattice modifies the properties of the cubic phase, removing their pure para-electric character.

Acknowledgments

The authors would like to thank Dr A Kania for growing the crystals and Dr J Dec for the control of the domain structure changes. One of us (KR) thanks the University of Metz for the hospitality and financial support.

References

Bauerle D, Holzapfel W B, Pinczuk A and Yacoby Y 1977 *Phys. Status Solidi* b **83** 99
Bauerle D and Pinczuk A 1976 *Solid State Commun.* **19** 1169
Bauerle D, Yacoby Y and Richter W 1974 *Solid State Commun.* **14** 1137
Dec J 1988 private communication
Fujishita H and Hoshino S 1984 *J. Phys. Soc. Japan* **53** 226
Handerek J, Kwapulinski J, Pawelczyk M and Ujma Z 1985 *Phase Trans.* **6** 35
Handerek J and Ujma Z 1977 *Acta Phys. Pol.* A **51** 87
Morozov E M, Smirnow V R, Klimow V V and Solovyev N C 1978 *Kristallografiya* **23** 119
Pasto A E and Condrate R A 1973 *J. Am. Ceram. Soc.* **56** 436
Roleder K 1980 *Acta Phys. Pol.* A **58** 623
—— 1988 *Ferroelectrics* **81** 1217
—— 1989 *Phase Trans.* at press
Roleder K and Dec J 1989 *J. Phys. Condens. Matter* **1** 1503
Roleder K, Kugel G E, Handerek J, Fontana M D, Carabatos-Nédelec C, Hafid M and Kania A 1987 *Ferroelectrics* **80** 809
Sawaguchi E 1953 *J. Phys. Soc. Japan* **8** 615
Scott B A and Burns G 1972 *J. Am. Ceram. Soc.* **55** 331
Tanaka M, Saito R and Tsuzuki K 1982 *Japan J. Appl. Phys.* **21** 291
Tennery V J 1965 *J. Electrochem. Soc.* **112** 1117
Ujma Z 1984 *Phase Trans.* **4** 169
Whatmore R W, Clarke R and Glazer A M 1978 *J. Phys. C: Solid State Phys.* **11** 3089
Zelezny V, Simon P and Gervais F 1988 *Ferroelectrics* **81** 865